

Article

Francis Type Turbine Runner Design and Comparison with Model Test Results

Buğra Yılmaz^{1,2}, Adnan Sözen^{1,*} and Oğuzhan Bendeş²¹ Energy Systems Engineering, Faculty of Technology, Gazi University, Ankara 06560, Turkey² TEMSAN, Türkiye Electromechanic Industry Corporation, Ankara 06200, Turkey* Correspondence: asozen@gazi.edu.tr; Tel.: 0090 312 202 8607**Received:** 8 December 2023; **Revised:** 25 January 2024; **Accepted:** 26 January 2024; **Published:** 23 February 2024

Abstract: Cavitation wear and hydraulic efficiency decrease in hydroelectric power plants have frequently been the subject of various research and studies. A hydroelectric power plant built on the Kızılırmak River in Türkiye started operating in 1960 and has not been subjected to any large-scale rehabilitation work other than general maintenance until today. The power plant has 4 Francis-type turbines, each with a power of 32 MW. Due to cavitation wear of turbine runners over the years, performance loss, vibration, and noise problems have arisen. Moreover, the maximum turbine hydraulic efficiency, which was 92% in 1960, the year the power plant was commissioned, decreased to 87.9% according to the efficiency measurements carried out at the power plant in 2020. In this study, Computational Fluid Dynamics (CFD) analyses were accomplished with Reynolds averaged Navier Stokes (RANS) calculations for the redesign of the Francis-type turbine runner and finally checked by a model test according to IEC 60193. It was observed that the model test and CFD results were close to each other, especially at the best efficiency point. The maximum turbine hydraulic efficiency, which was calculated as 94.95% as a result of CFD analysis at the nominal head, was calculated as 95.19% by the model test. The x-blade shape created in the redesigned turbine runner blades ensured homogeneous pressure distribution and increased the hydraulic efficiency significantly.

Keywords: computational fluid dynamics; Francis turbine runner design; hydroelectric power plant rehabilitation

1. Introduction

Today's socioeconomic developments increase the energy demand [1]. The increasing need for electrical energy in the world constantly directs people to alternative energy sources. There are various studies to increase the use of renewable energy resources [2].

Hydroelectric energy still has the highest capacity in the production ranking considering renewable energy sources in Türkiye. In addition, hydroelectric power plants have the lowest operating costs, longest operating life, and highest efficiency compared to other generation types [3].

Although the power plant mentioned in this study is one of the first power plants commissioned in Türkiye, it has not been the subject of a comprehensive rehabilitation study to date. The existing turbine runner blades in the power plant are conventional runner blades, and this type of blade causes cavitation damage, especially on the suction side of the runner blades [4]. There is also cavitation wear on the suction sides of the turbine runner blade surfaces in the power plant (Figure 1). There has been a serious decrease in the hydraulic efficiency value of this power plant over the years. According to the turbine manufacturer's information, the maximum turbine efficiency was 92% in 1960, the year the power plant was commissioned, decreased to 87.9% at a nominal head of 60 m and 51 m³/s flow rate according to the efficiency measurements fulfilled in the power plant in 2020 [5].

For these reasons, the turbine runners in this power plant needed to be redesigned, model-tested, manufactured, assembled, and commissioned in the power plant.



Figure 1. Existing runner of power plant.

The aim of the study was to design and model test a turbine runner that will reach high efficiency and homogenous pressure distribution. Another target was for the turbine to produce high mechanical power as a result of the high hydraulic efficiency achieved.

In this study, the CFD method was used together with RANS calculations for the redesign of the Francis turbine runner. The redesigned turbine runner blades were designed as an x-blade shape due to their advantages (Chapter 4.2).

During CFD studies, it was necessary to comply with the spiral case and draft tube dimensions, which cannot be revised because they are embedded in the concrete in the power plant. For this reason, 2D drawings in the power plant were used when creating 3D models of these existing parts. Laser scanning processes also helped create 3D models. After the runner design was completed, the turbine parts whose mesh structures were created were solved in ANSYS commercial software. As a result of CFD studies, a maximum hydraulic efficiency value of 94.95% was achieved and a homogeneous pressure distribution was obtained on the runner blade surfaces. After the CFD studies were completed, the redesigned turbine runner was manufactured at the model test scale and the model test was performed in accordance with the IEC 60193 standard [6].

In consequence of CFD analysis and model test, it was revealed that the turbine runner redesigned with the CFD method achieved similar results with the model test at the best efficiency point. In addition, according to both CFD and model test results, an increase of more than 7% was observed in the current maximum hydraulic efficiency value of the power plant. In addition, unlike the existing runner, which did not have a homogeneous pressure distribution and caused cavitation wear, the redesigned turbine runner was seen to have a homogeneous pressure distribution. The turbine runner designed with the CFD method was examined at the best efficiency point and no vortex that could cause a negative effect on its outlet section was observed. Likewise, no vortex formation was observed during the model test at the best efficiency point, extending to the draft tube walls and causing vibration.

The hydroelectric power plant operates at a flow rate between 40–60 m³/s and 60 m net head. The general features of the power plant are shown in Table 1.

Table 1. General features of the power plant.

Nominal Net Head	60	m
Maximum flow rate	61	m ³ /s
Rotational speed of turbine	187.5	rpm
Specific speed (n_q)	64.4	-
Turbine axis level	785.9	masl
Tail water level	784.2	masl
Number of turbine runner blades	13	#
Number of guide vanes	24	#

2. Current Studies in the Literature

Özcan [7] analyzed a Francis-type turbine runner using the CFD method with the help of ANSYS commercial software. As a result of the analysis, he proposed a design that he claimed was better in terms of energy production performance. In his study, he discussed the redesign process of the Francis turbine runner in a hydroelectric power plant with an installed capacity of 56 MW, built in 1973. The redesigned turbine runner was in the form of a x-blade and better flow conditions were obtained by reducing the angle at the runner shroud. Compared to the existing turbine in the power plant, the redesigned new runner showed that the best efficiency point was shifted from 37 m³/s-124 m to 39.5 m³/s-132 m. He also stated that the maximum efficiency of the turbine increased from 92.5% to 94.2% with the new design.

Benigni et al. [8] stated that the Meitingen hydroelectric power plant, built in 1922, was redesigned and produced due to cavitation damages, and with its installation, an annual production increase of 14.8% was achieved. ANSYS commercial software was used during the studies. In order to understand the different factors affecting turbine performance and get faster results, a simplified single-channel model was used, and inlet boundary conditions were determined at the guide vane entrance. Only one guide vane passage and one runner blade passage were used with periodic interfaces. Outlet boundary conditions were set to the draft tube outlet. In the second step, a general machine model was calculated and boundary conditions were placed at the real input. Thus, both guide vane and runner blade became 360-degree models. It was said that the highest efficiency of the existing turbine measured in the hydroelectric power plant was approximately 82.5%, and a turbine efficiency of 89.9% was achieved with the new design. They stated that as a result of the studies, electricity production increased by 14.8%, corresponding to an additional production of 10.74 GWh.

Celebioglu et al. [9] worked on CFD based rehabilitation procedure involving the redesign of the turbine of a hydroelectric power plant with the help of ANSYS commercial software. The study was performed on the redesign of the turbine runner in the Kepez-1 hydroelectric power plant in Türkiye. It was stated that the Francis turbine in the Kepez-1 hydroelectric power plant operates at a maximum efficiency of 92%. It was emphasized that noise, vibration and cavitation problems occurred in the existing Francis type turbine in the power plant and therefore a new runner design was developed. They stated that with the new design, the turbine reached the highest efficiency of 94.54% without disc friction losses. It was reported that no negative situation was observed in the runner blades' pressure loading graphs. The authors emphasized the importance of not only technical drawings but also laser scanning processes accomplished at the power plant in rehabilitation projects. Another result was that the blade form designed in the x-blade form instead of the traditional runner blade geometry provided an increase in power and efficiency results.

3. Studies to Create 3D Models

Before starting the design and CFD analysis of the Francis-type turbine runner of the hydroelectric power plant, 3D models were created in the commercial software Autodesk Inventor program. Model drawings were based on 2D drawings and scanned the surfaces of the turbine components by means of laser scanner. The newly designed Francis turbine runner was designed to adapt to the existing spiral case, stay vanes and draft tube in the power plant, which could not be replaced.

Power plant turbines have a spiral case that distributes pressurized mass flow to the runners in a circumferential manner. For good turbine performance, the distribution of kinetic energy and pressure energy is provided by the spiral case [10]. The inlet diameter of the spiral case was 3550 mm. The function of stay vanes mounted on the spiral case with welded manufacturing is to direct the water to the runner. The height of stay vanes was 765 mm. The 3D model of the spiral case and stay vanes of the hydroelectric power plant is shown in Figure 2.



Figure 2. Spiral case and stay vanes 3D model.

There were 24 guide vanes in one unit to adjust the direction and mass flow passing through the stay vanes. The height of the guide vanes was 765 mm, and this measurement was also the mass flow inlet height of the turbine runner. The guide vane designed for the power plant is shown in Figure 3.

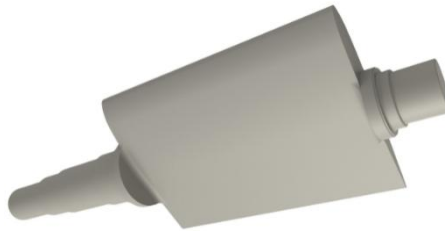


Figure 3. Guide vane designed for power plant.

In hydroelectric power plant turbines, there was a draft tube that allowed the depressurized discharge flow rate coming out of the runner to be directed to the tail water. The mass flow inlet part of the draft tube was a conical pipe and the inlet diameter was 3277 mm. At the exit of the draft tube, two outlet sections of 3500×4500 mm open to the tailwater field. The 3D model of the draft tube is shown in Figure 4.



Figure 4. 3D model of the draft tube.

4. Materials and Methods

In this study, the CFD method was used to redesign the Francis turbine runner and then model test of the redesigned turbine runner was carried out in accordance with the IEC 60193 standard. Firstly, a redesigned runner was created with the CFD method, using the characteristics of the turbine in the power plant that would remain the same, such as flow rate, head, and turbine speed. Then, the model test was performed by manufacturing the runner reduced to the model test scale.

CFD is a computer-based tool that can also be used to simulate the flow behavior of hydraulic machines [11]. CFD method provides the opportunity to evaluate the regional characterization of turbines such as regional pressure distribution, speed changes, and pressure fluctuations. Within the scope of CFD studies, ANSYS 18.1

commercial software [12] was used and its main Workbench, Design Modeler, Bladegen, Turbogrid, Meshing, ICEM CFD and CFX modules were utilized.

The solutions were realised with the help of Reynolds averaged Navier-Stokes (RANS) equations. Navier-Stokes equations describe the partial differential equations of a viscous, incompressible fluid and are part of the principle of conservation of momentum, mass and energy.

4.1. Specific Speed Calculation

The hydraulic properties of the power plant were used to calculate the specific speed (n_q) at the best efficiency point of the turbine, which is one of the basic parameters of turbine runner design. Specific speed is a function of flow rate and pressure in hydraulic machines. It was evaluated that the best hydraulic efficiency point of the turbine at a flow rate corresponding to 90% of the maximum flow rate. Since the rotation speed of the turbine runner was 187.5 rpm, the specific speed was calculated as 64.4 (Equation (1)).

$$n_q = n \times \frac{\sqrt{Q_{Best\ Eff.\ Point}}}{(H_{net})^{0.75}} = n \times \frac{\sqrt{0.9 \times Q_{Runner, Max}}}{(H_{net})^{0.75}} = 187.5 \times \frac{\sqrt{0.9 \times 61}}{(60)^{0.75}} = 64.4 \quad (1)$$

4.2. Turbine Runner Design and Optimization

The design of the turbine runner blades was finalized in the Bladegen module of the ANSYS commercial software. In the Bladegen module, the blade design of the runner was fulfilled to comply with the existing spiral case and draft tube dimensions in the power plant. The most challenging process in turbine design was runner design [12]. During the runner blade design, optimization studies were achieved using appropriate values for beta and theta angles. As a result of these optimizations, the runner blade design that gives convenient hydraulic efficiency and cavitation values was determined as the final design, and analyses were carried out on the flow rate and head values in the working range. The beta angle at the turbine runner inlet was set between 59° (shroud side) and 75° (hub side). On the other hand, the runner blade beta angle at the outlet varied between 5.7° (shroud side) and 51° (hub side).

Figure 5 shows the distribution of theta angles in meridional length used for 21 spans on the runner blades. The “theta beginning” option selected in the Bladegen module also helped create the x-blade shape. Unlike the traditional Francis runner design, the leading edge of the x-blade runner blades was inverted and the trailing edge was crooked. Thanks to this design, a highly balanced flow area was created in the runner passageways and a homogeneous pressure distribution was achieved on the runner blades [4]. This process also helped to achieve a more even pressure distribution on the turbine runner [13].

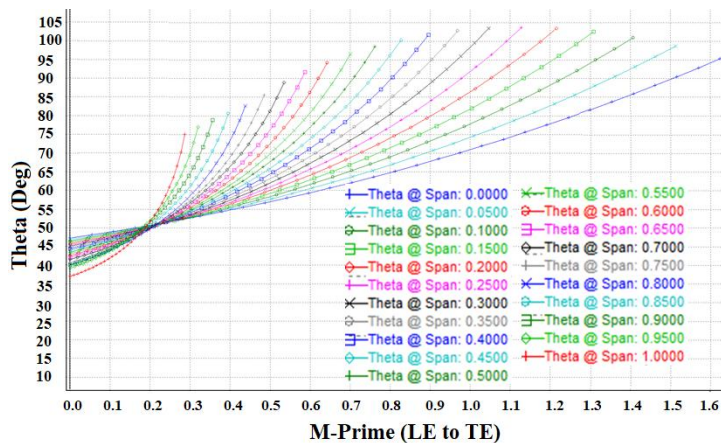


Figure 5. Runner blades theta angle distribution.

During the optimization of the Francis turbine runner, characteristic features such as meridional view and blade angles were changed, thus, the efficiency value was shifted to the desired flow rate value. Then, the performance of the most suitable blade design was analyzed using the full turbine CFD model and the results were evaluated. Figure 6 shows the redesigned runner blade meridional view and 3D visual of the runner.

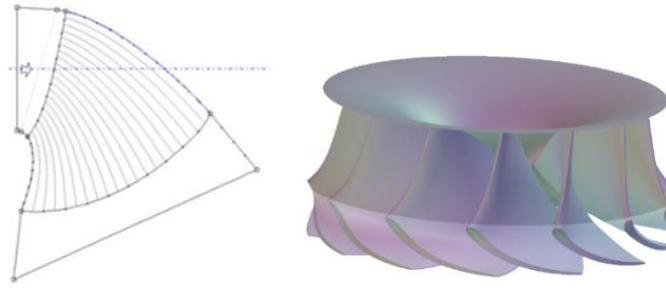


Figure 6. Meridional cross-section view (left) and 3D view (right) of the redesigned runner.

4.3. The Meshing of Components

Guide vane and runner blade meshes were created in the TurboGrid module of ANSYS commercial software. Spiral case, draft tube and tail water block meshes were created in the ICEM CFD module. Mesh sizes (fine mesh) of the components [14] in the full turbine model are shown in Table 2. Mesh structures of redesigned runner blades are shown in Figure 7.

Table 2. The mesh size of full turbine model components.

Areas	Nodes	Elements
Spiral Case	2.682.004	6.656.724
Guide Vanes	9.528.480	9.074.688
Runner	7.439.380	6.991.296
Draft Tube	7.190.880	7.120.365
Tail Water Block	833.000	813.606
Total	27.673.744	30.656.679

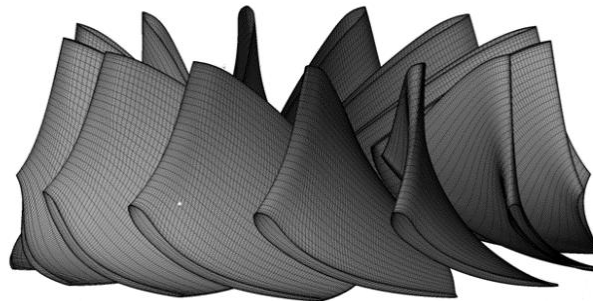


Figure 7. Mesh image of redesigned runner blades.

4.4. CFD Analysis Setup Settings

During the studies, firstly, CFD analyses of the turbine in the power plant were wanted to be carried out. However, the current 3D model of the runner could not be created because some of the turbine runner detailed projects did not provide appropriate storage conditions and were corroded over time. For this reason, 3D scanning of the existing runner was attempted, but since the runner was not disassembled and the laser scanning device could not reach the runner inlet part, this part could not be scanned and a 3D model of the runner could not be created. During the studies, CFD analyses of the existing runner could not be performed, so the studies started with the process of designing a new runner.

Flow analyses were performed for steady state with the help of the CFX module of ANSYS commercial software. Steady-state analyses were achieved using the Shear Stress Transport (SST) turbulence model [15]

developed by F. R. Menter. In the analysis, total pressure was defined at the spiral case inlet, and constant static pressure was defined at the tail water block outlet.

The simple model [8] did not include the spiral case, it contained a single guide vane and a single runner blade, provided that periodic boundary conditions were used together with the draft tube. It was assumed that the mass flow enters the guide vane at an angle of 40° , which was the exit angle of the spiral case stay vanes. The simple turbine model was used to obtain faster results from different designs and to finalize optimization studies. The runner optimization process was accomplished in the simple turbine model and the final results were achieved by solving the full turbine analysis. The simple model is shown in Figure 8. Simple model analyses were only a guide for the studies and the analysis results created with the simple setup were not used in the numerical and visual results given in this study.

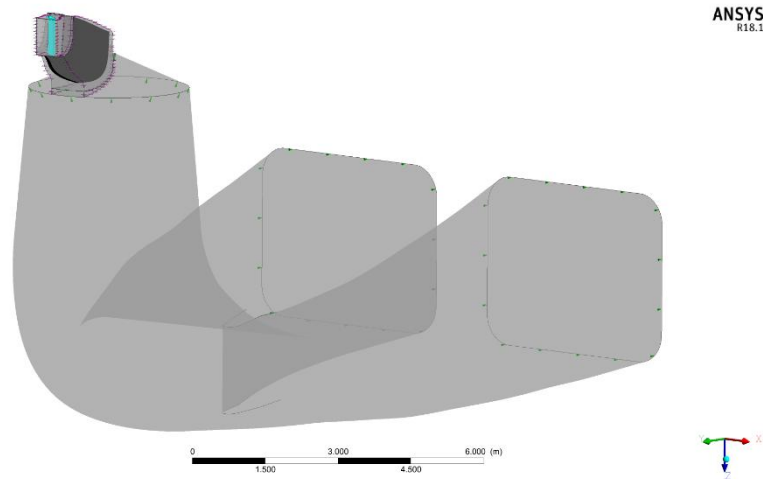


Figure 8. Simple model.

The full turbine model (Figure 9) was created by using interface models to ensure that the flow reaches the tailwater block without loss from the spiral case inlet. Unlike the simple model, a 360° turbine model was used in the full turbine model. In this model, the full turbine model was created by duplicating the guide vane 24 times and the runner blade 13 times. Each passage was connected to the next passage with a 1:1 interface. For the steady state and single-phase simulation, the “frozen rotor” interface type was used at the transition from the guide vanes to the runner and from the runner to the draft tube. This interface type allowed the relative allocation of rotating and stationary domains to be frozen during the simulation. The components in the full turbine model were the spiral case, guide vanes, runner, draft tube and tail water block, from the mass flow inlet to outlet, respectively. The tailwater block was used to prevent outlet boundary conditions from occurring directly at the outlet of the draft tube [16]. All numerical and visual values stated in this study show the results of full turbine analyses.

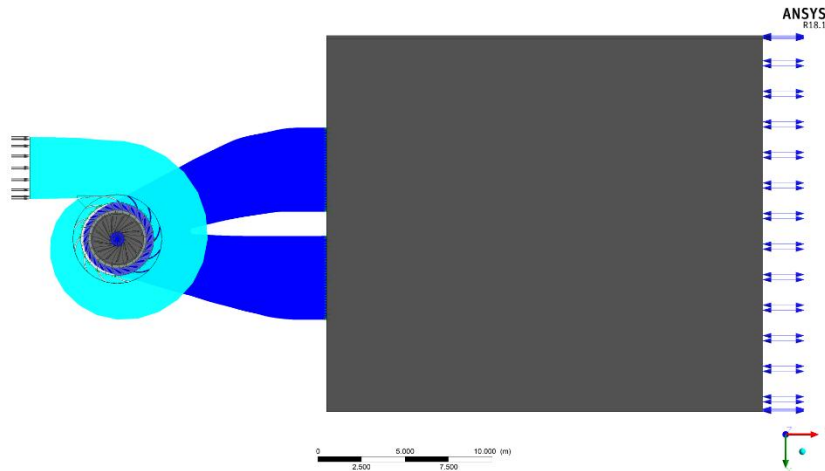


Figure 9. Full turbine model.

During the analyses, the runner domain was rotating at 187.5 rpm. Other components of the turbine were set stationary. Turbulence intensity was 5% in all analyses.

Numerical analyses were accomplished with the help of Navier-Stokes equations in the CFX module of the ANSYS commercial software used during the studies. These equations allowed describing fluid motions in 3 dimensions and were used together with the RANS formulation [4].

The values for the boundary conditions at the inlet and the outlet are shown in Tables 3 and 4. The pressure differences of 689.725 Pa and 101.325 Pa are approximately equivalent to a net head of 60 m.

Table 3. Inlet boundary conditions.

Inlet	Spiral Case
Features	The total pressure, flow direction: normal to the boundary, medium turbulence intensity, and Eddy viscosity ratio
Pressure	689.725 (Pa)

Table 4. Outlet boundary conditions.

Outlet	Outblock
Features	Static pressure, flow direction: normal to the boundary, medium turbulence intensity, and Eddy viscosity ratio
Pressure	101.325 (Pa)

4.5. Mesh Independence Study

Mesh independence studies were also performed during CFD studies and conducted with 4 different mesh element values for 60 m head and 20° guide vane openings for each mesh number of elements. These meshes were named coarse, medium, fine, and very fine. The total number of elements [14] for these mesh values is shown in Figure 10. During these studies, 94.94% hydraulic efficiency and 57.6 m³/s flow rate for coarse mesh, 95.34% hydraulic efficiency and 54.6 m³/s flow rate for medium mesh, 95.67% hydraulic efficiency and 54.5 m³/s flow rate for fine mesh, 95.76% hydraulic efficiency and 54.5 m³/s flow rate for very fine mesh values were achieved (Figure 11). Labyrinth and disk friction losses were not considered during mesh independence studies. These results were evaluated and a very small, negligible efficiency difference could be detected between the fine and very fine mesh sizes [14]. So full turbine analyses were performed at the fine mesh due to the advantages of the number of elements.

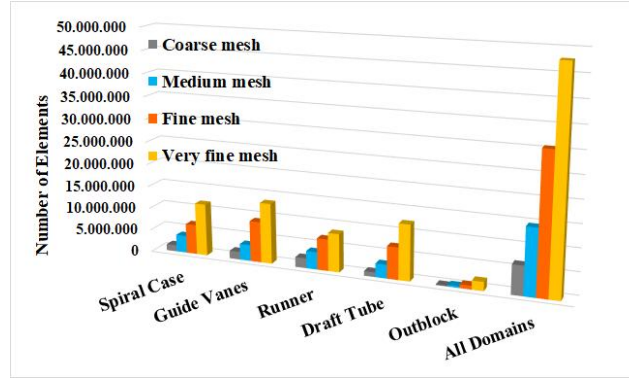


Figure 10. Mesh sizes used for mesh independence study.

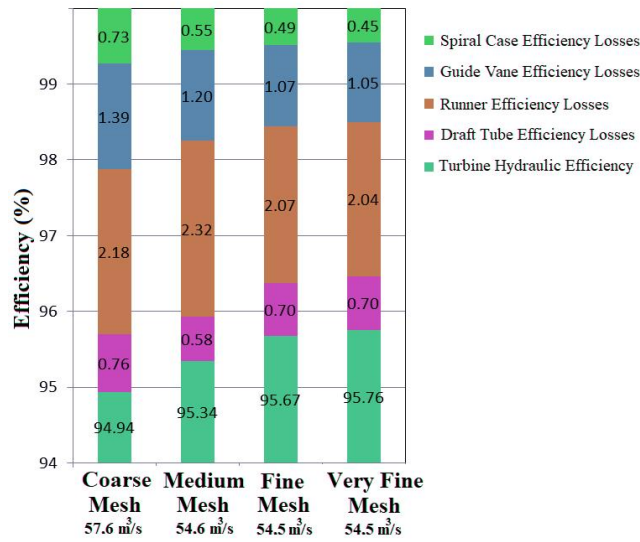


Figure 11. Loss compositions for different mesh numbers.

4.6. CFD-Post Evaluation Equations

During the CFD-post study, turbine characteristic results were evaluated in accordance with the IEC 60193 standard. In order to evaluate the turbine performance, the net head [16] and hydraulic efficiency of the turbine were calculated with Equation (2) [8] and Equation (3). In order to evaluate the performance of each component of the turbine, head loss calculation [4] was also carried out with Equation (4). This approach allowed us to evaluate the losses occurring in each component.

$$H_{net} = \frac{\left(p_{Spiral,in} + \frac{\rho \times v_{in}^2}{2} \right) - \left(p_{Drafttube,out} + \frac{\rho \times v_{out}^2}{2} \right)}{\rho \times g} \quad (2)$$

$$\eta_{hydr.} = \frac{\text{Mechanical power output}}{\text{Hydraulic power}} = \frac{T_{(z)@RU} \times \omega}{\rho \times g \times Q \times H_{Net}} = \frac{(T_{(z)@Blade} + T_{(z)@Hub} + T_{(z)@Shroud}) \times \frac{2 \times \pi \times r}{60}}{\rho \cdot g \cdot Q \cdot H_{Net}} \quad (3)$$

$$\eta_{hydr.} = 1 - \frac{\sum H_{Loss}}{H_{Net}} = 1 - \frac{H_{Loss,Spiral} + H_{Loss,Guidevane} + H_{Loss,Runner} + H_{Loss,Drafttube}}{H_{Net}} \quad (4)$$

H_{net} , defined as net head, was calculated directly from the total pressure difference at the spiral case inlet and draft tube outlet. Flow velocities at the inlet and outlet are also included in the calculations as well. While calculating hydraulic efficiency, a classical approach, the ratio of mechanical power to hydraulic power, was used.

Hydraulic power was calculated from the potential energy of mass flow, whereas the torque values of the runner components resulting from the CFD method were used when calculating the mechanical power. Multiplication of rotational torque by angular velocity indicated the mechanical power.

5.CFD Results

Steady-state CFD analyses of the full turbine model were solved with fine mesh and the results were examined. Leakage and disc friction losses in CFD analyses were taken from the IEC 62256 standard as a function of the specific speed n_q (Figure 12). The IEC 62256 standard [17] provides standards for the rehabilitation and performance improvement of hydraulic turbines, storage pumps and pump turbines. It appeared that the combined losses of a Francis turbine runner with a n_q of approximately 65 may be around 1%. This loss value was taken into account in the calculation of the total hydraulic turbine efficiency calculated with the CFD model.

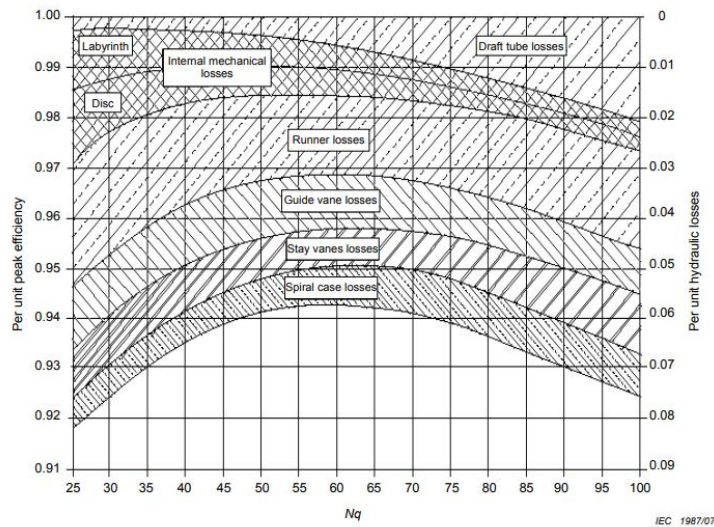


Figure 12. Losses from hydraulic turbine components according to IEC 62256 standard.

Efficiency values created by considering the operating points were examined. It was observed that the turbine reached the highest hydraulic efficiency at 60 m head and 55 m³/s flow rate. The hydraulic turbine efficiency value reached 60 m head and 55 m³/s flow rate, which was called the best efficiency point, was 94.95%. As a result of CFD analyses, the hydraulic efficiency values reached the nominal head and flow rate values of 40, 48, 55, and 60 m³/s are shown in Table 5.

Table 5. Turbine hydraulic efficiency values at nominal head according to CFD analysis results.

Head (m)	Flow Rate (m ³ /s)	Hydraulic Efficiency (%)
60	40	89.88
60	48	93.13
60	55	94.95
60	60	94.26

The blade loading chart occurred in each span of the runner blades at 60 m head and 55 m³/s flow rate, which was the best efficiency point of the design, is shown in Figure 13. Runner pressure contours are shown in Figure 14. At the best efficiency point, an almost homogeneously decreasing pressure distribution was observed on the suction and pressure sides of the runner blades from the mass flow inlet to the outlet, and there were no negative pressure zones on the runner surfaces. At the same time, it was observed that the runner could work with higher efficiency in a wider working range with better cavitation performance with the x-blade form realized with the new design [18].

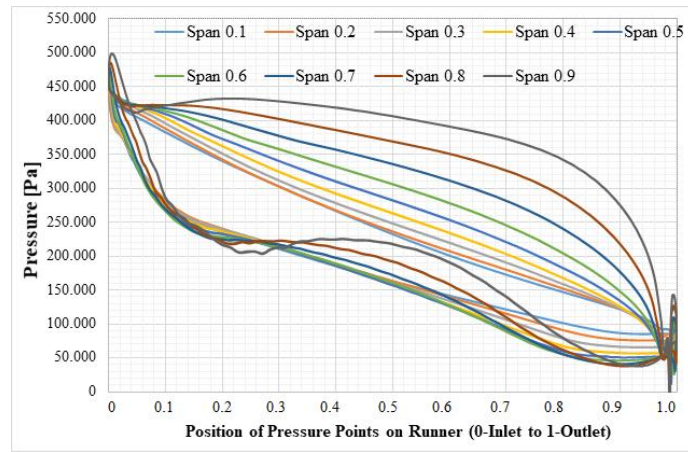


Figure 13. Blade loadings of runner blades at 60 m head and 55 m³/s flow rate as a result of CFD analysis.

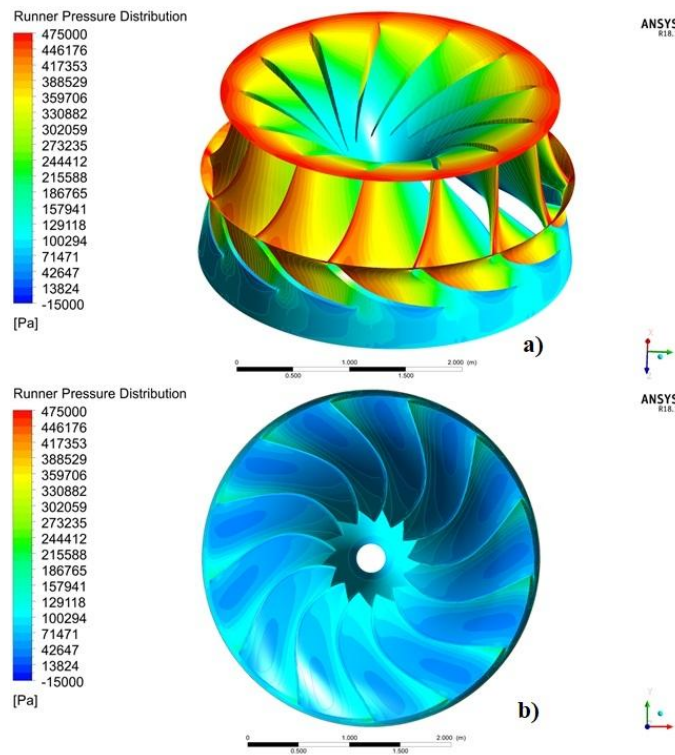


Figure 14. Turbine runner pressure distribution as a result of CFD analysis at 60 m head and 55 m³/s flow rate (a) isometric view; (b) bottom view.

Vortex ropes at the runner outlet were also examined at the best efficiency point and no vortex ropes extending to the draft tube walls were observed at the runner outlet (Figure 15).



Figure 15. Runner outlet vortex rope at 60 m head and 55 m³/s flow as a result of CFD analysis.

6. Model Test Results

The model test of the redesigned turbine runner was accomplished in the Graz University of Technology Institute of Hydraulic Fluid Machinery Laboratory in accordance with the IEC 60193 standard. The IEC 60193 standard provides standards for model acceptance tests of hydraulic turbines, storage pumps and pump turbines, and accordingly, for the model test of Francis turbines, the smallest value of the model runner diameter should be 250 mm (Table 6). The runner diameter of the turbine for which the model test was carried out was 340 mm.

Table 6. Minimum requirements for the model runner according to IEC 60193 standard.

Parameter	Type of Machine			
	Radial (Francis)	Diagonal (Nuxed-flow)	Axial (Kaplan, bulb)	Impulse (Pelton)
Reynolds Number <i>Re</i> (-)	4×10^6	4×10^6	4×10^6	2×10^6
Specific Hydraulic Energy (per stage) <i>E</i> (J·kg ⁻¹) ^{a)}	100	50	30 ^{b)}	500
Reference Diameter <i>D</i> (m)	0.25 ^{c)}	0.30	0.30	-
Bucket Width <i>B</i> (m)	-	-	-	0.08

a) With respect to the Froude similitude condition, the test specific hydraulic energy for cavitation tests may be chosen so that the resulting *Re* number is lower than the value given.

b) $E_{min} = 20 \text{ J} \cdot \text{kg}^{-1}$ if $D \geq 0.4 \text{ m}$.

c) For pumps and pump-turbines with low specific speed, a reference diameter such as $0.20 \text{ m} \leq D \leq 0.25 \text{ m}$ may be allowed if the outer diameter is equal to or greater than 0.5 m.

The turbine runner redesigned by the CFD method and the model turbine runner used in the model test are shown in Figure 16.

During the model test, the static pressure difference between the turbine inlet and outlet was measured and the turbine net head was determined. The inlet pressure was measured from four points circumferentially from the inlet of the spiral case, and the outlet pressure was measured from the outlet of the draft tube [19]. The DN250 flow meter was used to measure the flow rate of the turbine.

A torque transducer was positioned on the turbine shaft for measurement of rotational speed and torque. Torque measurement was performed by measuring the angular deviation of the shaft, and speed measurement was carried out by the infrared method.

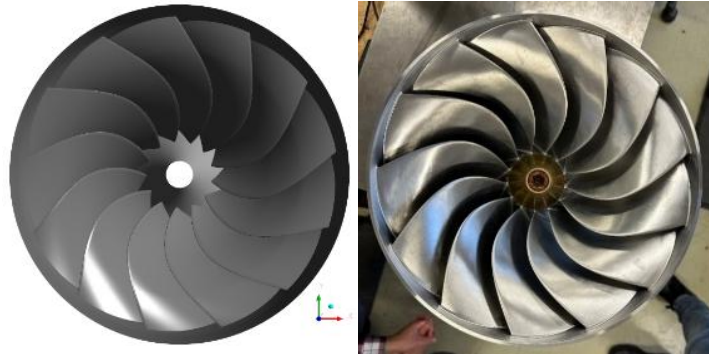


Figure 16. Redesigned runner with CFD (left) and the runner used in the model test (right).

According to the model test results, the hydraulic efficiency values achieved at 60 m head are shown in Table 7. The hydraulic efficiency of the model turbine was measured as 95.19% at 60 m head and 55 m³/s flow rate, which was found to be the best efficiency point in CFD studies. The comparative graph of flow-dependent hydraulic efficiency values based on CFD analysis and model test results is shown in Figure 17.

Table 7. Turbine hydraulic efficiency values at nominal head according to model test results.

Head (m)	Flow Rate (m ³ /s)	Hydraulic Efficiency (%)
60	40	91.61
60	48	93.92
60	55	95.19
60	60	94.12

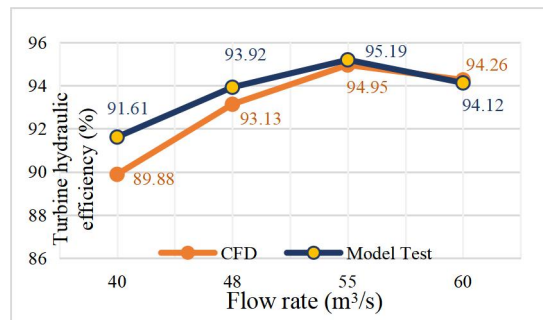


Figure 17. CFD and model test turbine hydraulic efficiency chart.

The draft tube cone used in the model test was made of transparent plexiglass material. Flow movements at the runner outlet are monitored with high-resolution cameras from this area. Vortex rope that may occur at the runner outlet from the draft tube transparent cone was examined and no vortex rope extending to the draft tube walls was observed at 60 m head and 55 m³/s flow rate, equivalent to the CFD analysis results (Figure 18).



Figure 18. Vortex rope occurring at the runner outlet at a 60 m head and 55 m³/s flow rate in the model test.

7. Discussion and Conclusions

In this study, the redesign and CFD analyses of a Francis-type hydraulic turbine runner with a specific speed value (n_q) of 64.4, which is currently in operation on the Kızılırmak River in Türkiye, were studied. The maximum efficiency value of the existing turbine in the power plant was measured as 87.9% as a result of the efficiency measurement performed in 2020. Moreover, the turbine runner was damaged by various abrasions since it has not been subject to large-scale rehabilitation work to date.

After the CFD studies model test of the redesigned runner was performed in accordance with the IEC 60193 standard and the results were evaluated. As a result of CFD analyses, the hydraulic efficiency of the runner at 60 m head and 55 m³/s flow rate, which was considered the best efficiency point, was found as 94.95% (Table 5). As a result of the model test, a hydraulic efficiency value of 95.19% was reached at the guide vane opening corresponding to the power plant's 60 m head and 55 m³/s flow rate (Table 7). The maximum efficiency value reached as a result of CFD studies and model tests was also found to be over 7% higher than the maximum hydraulic efficiency value of the original turbine existing in the power plant.

By evaluating the CFD analyses and model test results, it was revealed that the two methods gave similar results at the 55 m³/s flow rate, where the best efficiency point was seen in the CFD analyses [20], and this result continued very close to each other up to the 60 m³/s flow rate. As flow rate values decreased from 55 m³/s, where the best efficiency point was seen in CFD analyses, to lower flow rates, the hydraulic efficiency difference tended to increase in favor of the model test. For example, while the hydraulic efficiency value obtained as a result of the model test at a flow rate of 55 m³/s was 0.24% higher than the hydraulic efficiency value obtained as a result of CFD analyses, this value was 0.79% higher at a flow rate of 48 m³/s and 1.73% higher at a flow rate of 40 m³/s (Figure 17).

At the best efficiency point, no vortex movements extending to the draft tube walls were observed at the runner outlet in both the CFD (Figure 15) and model test results (Figure 18).

Evaluating the CFD and model test studies carried out in this study together, the following conclusions can be drawn;

- The performance results within operating ranges, other than the best efficiency point, in the Francis-type turbine runner design realised with the CFD method, still needs to be verified with experimental methods, however, the CFD method is a reliable way to reveal the best efficiency point of Francis turbine runner.
- The use of an x-blade type runner blade instead of conventional runner blade forms in the Francis turbine improves the turbine's hydraulic efficiency and pressure distribution.
- In addition to experimental studies, another reliable way to detect Francis turbine vortex ropes at the best efficiency point is the CFD method.

In future works, the turbine runner, which was redesigned and model tested within the scope of this study, is planned to be manufactured, assembled at the power plant, and put into operation. The performance level of the turbine runner will be measured on-site by the IEC 60041 standard [21] and thus its final verification will be achieved.

CFD method is a frequently used method today to evaluate the performance of hydraulic turbines. Although it is more time-consuming and costly compared to CFD analyses [22], it is still considered that the most reliable way to evaluate turbine performance is through experimental methods [12].

Acknowledgments

All authors would like to express their gratitude to TEMSAN, Türkiye Electromechanical Industry Corporation, which provided technical support to this study by sharing information and documents.

Conflicts of Interest

The authors claim that the publication of this review has no conflict of interest.

Nomenclature

CFD Computational Fluid Dynamics

RANS	Reynolds Averaged Navier Stokes
BEP	Best Efficiency Point
SST	Shear Stress Transport
IEC	International Electrotechnical Commission
Masl	Meters Above Sea Level (m)
GWh	Gigawatt hours
n_q	Specific speed
n	Rotational speed (rpm)
η	Efficiency (%)
η_{hydr}	Hydraulic efficiency (%)
Q	Flow rate (m ³ /s)
H_{net}	Net head (m)
H_{Loss}	Loss in meters (m)
P_{spiral}	Spiral case pressure (Pa)
$P_{Drafttube}$	Draft tube pressure (Pa)
ρ	Density (kg/m ³)
v	Velocity (m/s)
g	Gravitational acceleration (m/s ²)
$T_{(z)}$	Torque on Z axis (Nm)

References

- Öymen, G. The role of renewable energy on sustainability (in Turkish). Istanbul Commerce University Journal of Social Sciences, **2020**, *19*, 1069–1087. [CrossRef]
- Ürün, E.; Soyu, E. An evaluation on renewable energy sources in Türkiye's energy production (in Turkish). Available online: <https://dergipark.org.tr/pub/dpusbe/issue/31354/345354>.
- Gökdemir, M., Kömürcü, M.İ.; Evcimen, T.U. Overview of hydroelectric energy and HEPP applications in Türkiye (in Turkish). Available online: <https://www.imo.org.tr/Eklenti/568,turkiyede-hidroelektrik-enerji-ve-hes-uygulamalarina-genel-bakispdf.pdf?0>.
- Benigni, H.; Schiffer, J.; Jaberg, H.; Özcan, A.Ö.; Duva, B.C.; Mosshammer, M. Rehabilitation of a Francis turbine using CFD and optimization techniques: A case study in Turkey. In Proceedings of the Hydro-International Conference and Exhibition, Bordeaux, France, 26–28 October 2015.
- HATCH. (2019). Energy efficiency in power generation, condition assessment report for Hirfanlı HPP (unpublished report) (H358793).
- International Electrotechnical Commission. *IEC 60193-Hydraulic turbines, storage pumps, and pump-turbines—Model acceptance tests*; International Electrotechnical Commission: Geneva, Switzerland, 2019.
- Özcan, A.Ö. Evaluation of the efficiency increment potential for francis turbines using CFD analysis. Master's thesis, Middle East Technical University, Ankara, 2016.
- Benigni, H.; Schiffer, J.; Jaberg, H. Refurbishment of twin Francis turbines—maximizing the annual production. *IOP Conf. Ser.: Earth Environ. Sci.* **2019**, *240*, 022036. [CrossRef]
- Celebioglu, K.; Aradag, S.; Ece, A.; Altintas, B. Rehabilitation of Francis turbines of power plants with computational methods. *Hittite J. Sci. Eng.* **2018**, *5*, 37–48. [CrossRef]
- Dahal, D.; Chitrakar, S.; Kapali, A.; Thapa, B.; Neopane, H. Design of spiral casing of Francis turbine for micro hydro applications. *J. Phys.: Conf. Ser.* **2019**, *1266*, 012013. [CrossRef]
- Kecel, S.; Yavuzcan, H.G.; Sözen, A. Examination of flow effects in Francis turbine models with different numbers of rotor blades. *Politeknik Dergisi.* **2017**, *20*(1), 241–249.
- Aylı İnce, Ü. E. Design of Francis type turbine using numerical methods, parameter optimization and development of the numerical infrastructure of model tests (in Turkish). Doctoral thesis. TOBB University of Economics and Technology, Ankara, Turkey, 2016. <https://gcris.etu.edu.tr/handle/20.500.11851/2158>.
- Brekke, H. Design, performance and maintenance of Francis turbines. *Glob. J. Res. in Eng. Mech. and Mechanics Eng.* **2013**, *13*(5), 28–40.
- TEMSAN, Türkiye Electromechanic Industry Corporation. (2022). Computational fluid dynamics report (unpublished report).
- Menter, F.R. Two-equation eddy-viscosity turbulence models for engineering applications. *AIAA J.* **1994**, *32*(8), 1598–1605. [CrossRef]

16. Benigni, H.; Schiffer-Rosenberger, J.; Penninger, G.; Weichselbraun, C.; Artmann, M.; Juhrig, L.; Becker, M.; Krappel, T.; Jaberg, H. Cavitation as a limiting factor for the empowering of a Kaplan turbine–CFD calculations, test rig results and operational experience. **2020**, 1–10.
17. International Electrotechnical Commission. *IEC 62256-Hydraulic turbines, storage pumps and pump-turbines – Rehabilitation and performance improvement*. International Electrotechnical Commission: Geneva, Switzerland, 2017.
18. Demers, A. (2009). Francis turbine “x-blade” technology. *Hydro News, Magazine of Andritz Hydro*. <https://www.scribd.com/doc/226004893/hy-hn15-en>.
19. TEMSAN, Türkiye Electromechanic Industry Corporation. (2023). Model test report (unpublished report).
20. Jošt, D.; Škerlavaj, A.; Morgut, M.; Mežnar, P.; Nobile, E. Numerical simulation of flow in a high head Francis turbine with prediction of efficiency, rotor stator interaction and vortex structures in the draft tube. *J. Phys.: Conf. Ser.* **2015**, 579, 012006. [[CrossRef](#)]
21. International Electrotechnical Commission. *IEC 60041-Field acceptance tests to determine the hydraulic performance of hydraulic turbines, storage pumps and pump-turbines*. International Electrotechnical Commission: Geneva, Switzerland, 1991.
22. Jain, S.; Saini, R.; Kumar, A. CFD approach for prediction of efficiency of Francis turbine. In Proceedings of the 8th International Conference on Hydraulic Efficiency Measurement, IIT Roorkee, India, 21–23 October 2010.



Copyright © 2024 by the author(s). Published by UK Scientific Publishing Limited. This is an open access article under the Creative Commons Attribution (CC BY) license (<https://creativecommons.org/licenses/by/4.0/>).

Publisher's Note: The views, opinions, and information presented in all publications are the sole responsibility of the respective authors and contributors, and do not necessarily reflect the views of UK Scientific Publishing Limited and/or its editors. UK Scientific Publishing Limited and/or its editors hereby disclaim any liability for any harm or damage to individuals or property arising from the implementation of ideas, methods, instructions, or products mentioned in the content.